Q-plates as higher order polarization controllers for orbital angular momentum modes of fiber

P. Gregg,[1] M. Mirhosseini,[2] A. Rubano,[3] L. Marrucci,[3] E. Karimi,[4] R. W. Boyd,[2,4] and S. Ramachandran[1,*]

[1]*Boston University, 8 St. Mary's St., Boston, Massachusetts 02215, USA*

[2]*Institute of Optics, University of Rochester, Rochester, New York 14627, USA*

[3]*Dipartimento di Fisica, Università di Napoli Federico II and CNR-SPIN via Cintia, 80126 Napoli, Italy*

[4]*Department of Physics, University of Ottawa, 25 Templeton, Ottawa, Ontario K1N 6N5, Canada*

**Corresponding author: sidr@bu.edu*

Received February 3, 2015; accepted March 2, 2015;
posted March 13, 2015 (Doc. ID 232541); published April 8, 2015

We demonstrate that a $|q| = 1/2$ plate, in conjunction with appropriate polarization optics, can selectively and switchably excite all linear combinations of the first radial mode order $|l| = 1$ orbital angular momentum (OAM) fiber modes. This enables full mapping of free-space polarization states onto fiber vector modes, including the radially (TM) and azimuthally polarized (TE) modes. The setup requires few optical components and can yield mode purities as high as ~30 dB. Additionally, just as a conventional fiber polarization controller creates arbitrary elliptical polarization states to counteract fiber birefringence and yield desired polarizations at the output of a single-mode fiber, q-plates disentangle degenerate state mixing effects between fiber OAM states to yield pure states, even after long-length fiber propagation. We thus demonstrate the ability to switch dynamically, potentially at ~GHz rates, between OAM modes, or create desired linear combinations of them. We envision applications in fiber-based lasers employing vector or OAM mode outputs, as well as communications networking schemes exploiting spatial modes for higher dimensional encoding.

OCIS codes: (050.4865) Optical vortices; (260.6042) Singular optics; (260.5430) Polarization; (060.4230) Multiplexing.
http://dx.doi.org/10.1364/OL.40.001729

Fibers supporting cylindrical vector beams or orbital angular momentum (OAM) modes have recently gained attention for realizing high-power fiber lasers [1,2], and for enabling digital signal processing free multimode communications [3]. While much progress has been made on fiber designs supporting a multitude of optical vortex modes [4–9], exciting (multiplexing) or reading (demultiplexing) the states has been achieved primarily by spatial light modulators (SLM) [3,6,10] or combinations of segmented and spiral phase or wave plates [11,12]. Given widespread current interest in the field, recent demonstrations of chip-based mode conversion schemes [13–15] may also be candidates, although the ability of such devices to excite pure fiber modes is undetermined. Common to all these techniques is the fact that they create free-space vector or OAM modes, which are assumed adequate for fiber coupling because of similar mode amplitude, polarization, or phase distributions to the corresponding modes in suitably designed fibers.

However, there are some crucial distinctions between fiber and free-space vortex modes, limiting the applicability of such techniques in creating desired fiber modes. As an example, in fiber, vortex modes exist in degenerate pairs (except for the TE and TM modes) that may be prone to mixing, even when the fiber is designed to stably propagate separate OAM orders [4]. An intelligent (de)multiplexing device could create arbitrary linear combinations of these pairs of modes at low loss and with low device complexity. More generally, for switching between different fiber-OAM states, the (de)multiplexing device would have to produce arbitrary linear combinations of *any* pair of degenerate states. Thus, the best device for coupling from free space or a chip to fiber vortex modes should have functionality similar to wave plates or polarization controllers (polcons) that can create any linear combination of the two degenerate polarization modes in a single-mode fiber (SMF), *and* allow dynamic, high speed altering of this combination.

Here we show that so-called q-plate devices for free-space vortex mode creation offer precisely this functionality, and hence are ideal candidates for (de)multiplexing OAM and vector modes of fibers [16,17]. We demonstrate switching among all allowed first-radial-mode-order vector modes as well as the fundamental modes of a fiber designed to stably propagate vortices, using a q-plate and a polcon, or pair of conventional wave plates. Pulse propagation tests reveal the capability of achieving mode purities as high as 29.9 dB. Furthermore, we show that the q-plate enables creation of arbitrary linear combinations of the degenerate OAM modes, disentangling birefringence-induced OAM mixing effects in fibers. Finally, we show that switching among desired first order OAM modes involves only tuning polcons, implying that this system could enable nanosecond time scale switching–feasible with electronic polcons, which would be immensely useful for networking functionalities in mode-division multiplexing schemes, as well as switching bases in higher dimensional quantum links.

Eigenmodes of weakly guiding fibers may be completely represented by a radial function, along with a helical phase term $\exp(il\varphi)$ which denotes the amount of OAM, $l \cdot \hbar$, each photon in the mode carries [18] and polarization state, $\hat{\sigma}^{\pm} = (\hat{x} \pm i\hat{y})/\sqrt{2}$, indicating left/right circular polarization, denoting the amount of spin angular momentum each photon carries. These modes fall into two categories: those with OAM and spin aligned, or of the same handedness, and those with OAM and spin anti-aligned. For a given absolute value of OAM, $|l|$, the modes with spin and OAM aligned are degenerate in wave vector, β, with each other, as are the modes with spin and OAM anti-aligned. The two sets are not degenerate with each other; this is the main distinction from free-space modes, where all four are degenerate. An obvious exception is the case of the fundamental $l = 0$ mode, for which only two degenerate polarization modes exist. A second, more significant, exception exists for $|l| = 1$: the spin-orbit anti-aligned $|l| = 1$ states (total angular momentum $j = l + s = 0$) do not exist as fiber modes, but rather specific linear combinations exist as TE and TM modes, which are not degenerate with each other. Thus, the first set of higher order modes is given by

$$\mathrm{OAM}^{\pm}_{1m} = (\hat{\sigma}^{\pm} e^{\pm i\varphi}) F_m(r) e^{i\beta_{\mathrm{OAM}} z}, \quad (1)$$

$$\mathrm{TE}_{0m} = (\hat{\sigma}^{+} e^{-i\varphi} - \hat{\sigma}^{-} e^{+i\varphi}) \frac{F_m(r)}{\sqrt{2}i} e^{i\beta_{\mathrm{TE}} z}, \quad (2)$$

$$\mathrm{TM}_{0m} = (\hat{\sigma}^{+} e^{-i\varphi} + \hat{\sigma}^{-} e^{+i\varphi}) \frac{F_m(r)}{\sqrt{2}} e^{i\beta_{\mathrm{TM}} z}. \quad (3)$$

Here (r, φ, z) are cylindrical coordinates, F_m is the radial field distribution, and m is the radial mode order. In contrast to conventional fibers, OAM supporting fibers feature sufficient splitting in β to allow stable propagation of the three classes of modes described by Eqs. (1)–(3). For the fiber used here [5], $m = 1$ in all cases, so we neglect further radial subscripts for brevity. Note that the $\mathrm{OAM}^{\pm}$ modes are degenerate; hence, their linear combinations are also modes, forming an $\mathrm{OAM}^{\pm}$ subspace, in analogy to the $\hat{\sigma}^{\pm}$ subspace of elliptical polarizations of the $l = 0$ mode of fiber or free space. We have shown that, just as birefringence from fiber loops can be used to make polcons for the $l = 0$ mode, loops of OAM carrying fiber can span this $\mathrm{OAM}^{\pm}$ subspace [19]. However, while a simple free-space (bulk) wave plate can also provide the same functionality for the fundamental mode, SLMs, spiral phase plates, and similar devices used thus far in OAM-based fiber experiments will *not* facilitate straightforward creation of arbitrary linear combinations of OAM states in fiber.

Such functionality is offered by q-plates, which couple the spin and angular momentum of light in free space [20]. A q-plate of topological charge q performs the following linear transformation:

$$q \cdot (A\hat{\sigma}^{+} + B\hat{\sigma}^{-}) = A\hat{\sigma}^{-} e^{i2q\varphi} + B\hat{\sigma}^{+} e^{-i2q\varphi}. \quad (4)$$

That is, a q-plate imparts orbital angular momentum of $2q$, with sign depending on the spin of the incoming beam. Inspection of Eq. (4) shows that, by controlling A and B (the incoming polarization state) and choosing $q = -1/2$, any state in the $\mathrm{OAM}^{\pm}$ subspace in Eq. (1) can be obtained. Similarly, the TE and TM modes can be generated with a linear input polarization ($A = \pm B$), and a $q = 1/2$ plate, or equivalently, a $q = -1/2$ plate, followed by a half-wave plate. Finally, fundamental mode excitation is achieved by tuning the bias of the q-plate to yield λ retardation [21]. Thus, a q-plate and two wave plates suffice to create all linear combinations of the $|l| = 0$ and 1 modes of fiber.

Our experimental setup (Fig. 1) uses a continuous wave (CW) and pulsed lasers for characterization, and includes a 50/50 tap for interference to reveal the phase of the output beams. A commercial in-fiber electronic polcon tailors the input polarization state seen by the q-plate, while for the $\lambda/2$ plate following the q-plate, we use two $\lambda/4$-plates in series, turning the $\lambda/2$-plate "on" or "off" by aligning or crossing their fast axes, respectively. Total measured input coupling losses at the test wavelength of 1530 nm were 3.1 dB for the fundamental modes, and 2.4 dB for the $\mathrm{OAM}^{\pm}$ and TE/TM modes. 1.4 dB of loss was from the q–plate and could be further reduced with AR coating. The remainder is from beam imperfections or size mismatches, which could be optimized further. The output, after 300 m of fiber propagation, is either sorted by circular polarization and interfered with a reference beam, or directed to a fast detector and oscilloscope for time domain measurements. The length of fiber under test is chosen to be 300 m to enable time-domain measurements, which require sufficient group delays between the modes to distinguish them at the output. Longer lengths may well have been used in the apparatus shown in Fig. 1, since we have previously shown that OAM states in vortex fibers can be as much as 20 dB pure after km-length propagation [3,22].

Figure 2(a) shows experimental images of the slightly defocused fiber output sorted into $\hat{\sigma}^{+}$ and $\hat{\sigma}^{-}$ components for different launch conditions using a CW laser. As the interference patterns of the fundamental $l = 0$ modes look the same regardless of polarization, only one is shown. Our observations match the predictions of Eqs. (1)–(3): for $\mathrm{OAM}^{\pm}$, we expect a bright ring in only one polarization, while we expect two rings of equal brightness in each polarization for TE/TM. Superposition with a reference beam in Fig. 2(b) reveals the phase structure of the modes. The $\mathrm{OAM}^{\pm}$ modes show spirals with one arm and a handedness that matches polarization orientation. The TE/TM modes show one-armed spirals anti-aligned with the circular polarizations, and as evident from Eq. (2), the TE constituent OAMs are out of phase by π, while for the TM mode, the arms originate at the same point.

To obtain a more quantitative metric for excited mode purity, a picosecond pulsed laser (3 dB bandwidth

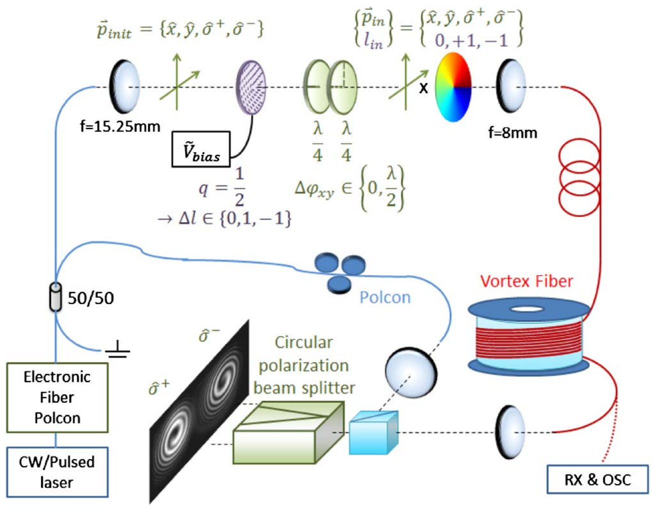

Fig. 1. Light with arbitrary uniform polarization from the electronic polcon passes through the q-plate and two quarter wave plates. The desired superposition of $|l| = 0$ or $|l| = 1$ modes is focused into the vortex fiber. The 50/50 tap provides a reference beam for interference measurements.

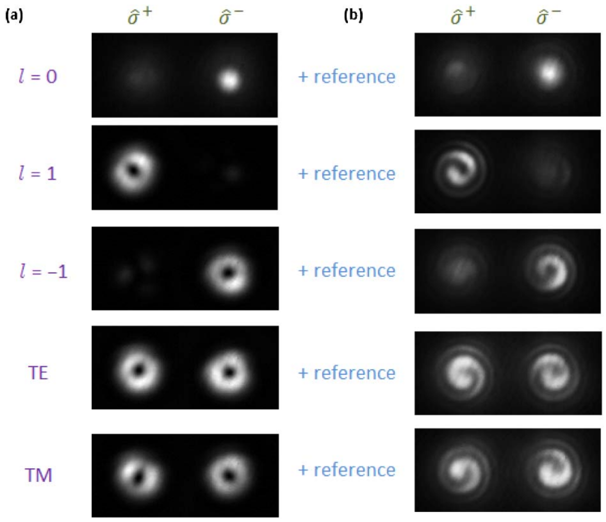

Fig. 2. (a) Output and (b) output, plus reference after propagation through 300 m of vortex fiber with a 1530 nm CW source for all modes of interest.

of 0.6 nm) at 1530 nm is used, and the fiber output is measured on a fast detector (New Focus 1444–50) and oscilloscope (Agilent 86100A, 40 GHz receiver). As each mode of interest possesses a unique group velocity, photons launched simultaneously into different modes will arrive at the detector at different times, except for degenerate mode pairs, which will arrive at the same time regardless of the mode excited within its subspace. Figure 3(a) illustrates this by exciting all modes when the coupling is intentionally misaligned. In addition to the $l = 0$, $\mathrm{OAM}^{\pm}$, and TE/TM modes, LP_{02} and LP_{21} exist in this fiber at 1530 nm [23], but they are inaccessible with the $q = -1/2$ plate and are considered parasitic for this experiment. When the fiber is aligned and one mode excited, the input coupling mode purity, or multipath interference (MPI) [24] between modes j and k, is calculated as

$$\mathrm{MPI} = 10 \log_{10}\left(\frac{P_{\mathrm{peak},j} - \bar{P}_{\mathrm{noise}}}{P_{\mathrm{peak},k} - \bar{P}_{\mathrm{noise}}}\right), \tag{5}$$

where $P_{\mathrm{peak},k}$ is the peak power of the kth mode, and $\bar{P}_{\mathrm{noise}}$ is the average noise power. The table in Fig. 3(b) shows MPI for selective excitation of each mode. Every resolvable measurement shows purity of at least −18 dB, indicating that any of the desired modes may be excited with high fidelity without displacing the fiber under test.

Having demonstrated the capability of exciting pure fiber modes with q-plates, we turn our attention to the ability of this system to excite arbitrary linear combinations of degenerate OAM fiber modes (Fig. 4). If the input polarization to the $q = -1/2$ plate is circular, and no coupling is observed in the fiber, the fiber output is a single OAM state [Fig. 4(a)]. That is, the fiber acts as a diagonal unitary matrix for the $\mathrm{OAM}^{\pm}$ subspace that does not couple power from OAM^{+} to OAM^{-}, or vice versa. However, once the fiber is subject to common perturbations such as bends and twists, degenerate state coupling occurs, and this is manifest in an OAM mode showing in both spin polarizations [Fig. 4(b)]. Thus, despite introducing a pure OAM^{+} or OAM^{-} mode at the input of the fiber, the output is an arbitrary state in this OAM subspace, i.e., the matrix is no longer diagonal. Note that just inspection of power in the two polarization bins suffices to draw this conclusion, because Eq. (1) indicates that the OAM state of polarization $\hat{\sigma}^{+}$ is necessarily OAM^{+} and the state with $\hat{\sigma}^{-}$ polarization is likewise only OAM^{-}. However, Eqs. (1) and (4) also show that both the fiber and q-plate span the same OAM subspace, meaning that the input state can be tailored by simply introducing a specific elliptical polarization to the q-plate, such that this state, after mixing in the fiber, again yields the desired pure OAM^{+} or OAM^{-} state at the fiber output [Fig. 4(c)].

In summary, a setup comprising a q-plate and two polarization controllers not only allows creation of all first radial order vortex modes in fibers, but also enables creating linear combinations of these modes, hence facilitating (a) switching between the modes within any specific $|l|$ subspace, by tuning the polcons alone (achievable at GHz rates [25]); or (b) disentangling of degenerate state mixing that may be unavoidable because of fiber perturbations. While creating the states, and to some extent, switching between a limited number of states, though not at GHz speeds, can be achieved by the multitude of other OAM excitation devices (e.g., SLMs), disentangling the effects of the fiber propagation is a functionality unique to fiber-bend induced polcons and the q-plate system we demonstrate here. Between the latter two devices, the q-plate system would be preferable to fiber bends for multiple reasons: in fibers that support multiple OAM modes, a series of fiber bends may not necessarily uniquely disentangle *all* degenerate OAM mode orders, and there is some indication that fiber bends may be increasingly ineffective as mode order increases [22]. Finally, we note that interferometric mode shaping techniques are always available for creating arbitrary mode shapes and polarization patterns. Several early experiments on creating radially polarized beams used such techniques [26,27], but none, to the best of our knowledge, have achieved the 18-30 dB

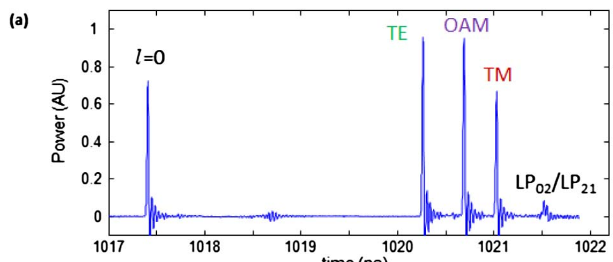

(b)

Excited\Meas	l=0	TE	OAM	TM	LP02/LP21
l=0	-	-24.6	-21.0	-24.2	-29.5
TE	-20.4	-	-19.1	-19.1	-13.8*
OAM	-22.9	-22.1	-	-18.8	-19.1
TM	-20.9	-29.9	-19.1	-	18.1

Fig. 3. (a) Time of flight measurement indicating different arrival times for different (non-degenerate) modes. (b) input coupling MPI in dB. Each row indicates the same desired mode. *MPI of TE into LP02/LP21 not resolvable below 13.8 dB due to detector impulse response.

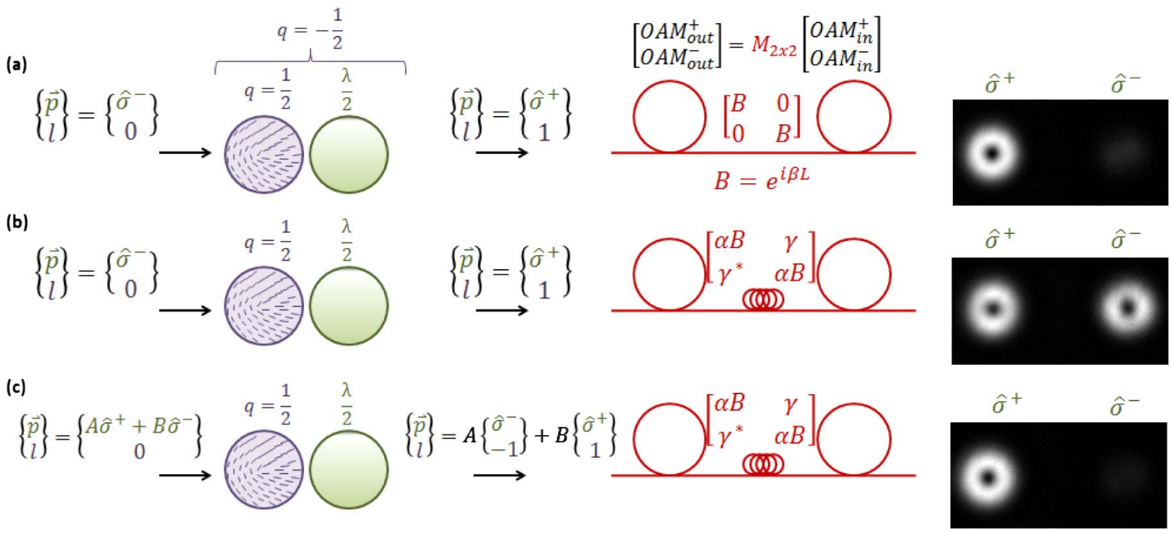

Fig. 4. OAM transmission schematic and experimental results, using a $q = -1/2$ plate (here comprised of a $q = 1/2$ plate and a half wave plate) in the case of (a) a fiber maintaining OAM state, (b) a fiber mixing degenerate OAM state according to some mixing coefficient, γ, with $|\gamma|^2 + |\alpha|^2 = 1$, and (c) a fiber mixing degenerate OAM states, but in which said coupling is accounted for by tuning the input polarization.

purity levels shown here, and none of them would be as alignment insensitive as this simple setup comprising, essentially, three wave plates in series. The q-plate based setup is similar to segmented wave plates [11] used for creating radially polarized beams, but with the added advantages of significantly improved OAM purity and tunability, and hence is capable of offering switchability and the aforementioned "unwrapping" of fiber mixing. Thus, we believe that the q-plate excitation scheme shown here would be applicable to the development of vector field output fiber lasers, and would play a role as vital as the polarization controller in SMF, for realizing quantum or classical communications links that aim to exploit spatial modes as a dimension in which to encode information.

The authors would like to thank P. Kristensen for help with fiber fabrication. This work was funded in part by the DARPA InPho program under grant nos. W911NF-12-1-0323 and W911NF-13-1-0103, and NSF grant no. ECCS-1310493. P.G. acknowledges support from NSF-GRP grant no. DGE-1247312. E. K. and R. B. would like to acknowledge the support of the Canada Excellence Research Chairs (CERC) program.

References

1. S. Piehler, X. Delen, M. Rumpel, J. Didierjean, N. Aubry, T. Graf, F. Balembois, P. Georges, and M. A. Ahmed, Opt. Express **21**, 11376 (2013).
2. M. Fridman, M. Nixon, M. Dubinskii, A. A. Friesem, and N. Davidson, Opt. Lett. **35**, 1332 (2010).
3. N. Bozinovic, Y. Yue, Y. Ren, M. Tur, P. Kristensen, H. Huang, A. E. Willner, and S. Ramachandran, Science **340**, 1545 (2013).
4. S. Ramachandran and P. Kristensen, Nanophotonics **2**, 455 (2013).
5. S. Ramachandran, P. Kristensen, and M. F. Yan, Opt. Lett. **34**, 2525 (2009).
6. C. Brunet, P. Vaity, Y. Messaddeq, S. LaRochelle, and L. A. Rusch, Opt. Express **22**, 26117 (2014).
7. Y. Yue, Y. Yan, N. Ahmed, J.-Y. Yang, L. Zhang, Y. Ren, H. Huang, K. M. Bimbaum, B. I. Erkmen, S. Dolinar, M. Tur, and A. Willner, IEEE Photonics. **4**, 535 (2012).
8. S. Li and J. Wang, Sci. Rep. **4**, 3853 (2014).
9. X. M. Xi, G. K. L. Wong, M. H. Frosz, F. Babic, G. Ahmed, X. Jiang, T. G. Euser, and P. St. J. Russell, Optica **1**, 165 (2014).
10. M. Mirhosseini, O. S. Magana-Loaiza, C. Chen, B. Rodenburg, M. Malik, and R. W. Boyd, Opt. Express **21**, 30196 (2013).
11. G. Machavariani, Y. Lumer, I. Moshe, A. Meir, and S. Jackel, Opt. Commun. **281**, 732 (2008).
12. D. Lin, J. M. O. Daniel, M. Gecevicius, M. Beresna, P. G. Kazansky, and W. A. Clarkson, Opt. Lett. **39**, 5359 (2014).
13. T. Su, R. P. Scott, S. S. Djordjevic, N. K. Fontaine, D. J. Geisler, X. Cai, and S. J. B. Yoo, Opt. Express **20**, 9396 (2012).
14. X. Cai, J. Wang, M. J. Strain, B. Johnson-Morris, J. Zhu, M. Sorel, J. L. O'Brien, M. G. Thompson, and S. Yu, Science **338**, 363 (2012).
15. J. Sun, M. Moresco, G. Leake, D. Coolbaugh, and M. R. Watts, Opt. Lett. **39**, 5977 (2014).
16. L. Marrucci, C. Manzo, and D. Paparo, Phys. Rev. Lett. **96**, 163905 (2006).
17. E. Karimi, B. Piccirillo, E. Nagali, L. Marrucci, and E. Santamato, App. Phys. Lett. **94**, 231124 (2009).
18. L. Allen, M. W. Beijersbergen, R. J. C. Spreeuw, and J. P. Woerdman, Phys. Rev. A **45**, 8185 (1992).
19. N. Bozinovic, S. Golowich, P. Kristensen, and S. Ramachandran, Opt. Lett. **37**, 2451 (2012).
20. L. Marrucci, E. Karimi, S. Slussarenko, B. Piccirillo, E. Santamato, E. Nagali, and F. Sciarrino, Appl. Opt. **53**, 1 (2012).
21. S. Slussarenko, A. Murauski, T. Du, V. Chigrinov, L. Marrucci, and E. Santamato, Opt. Express **19**, 4085 (2011).
22. P. Gregg, P. Kristensen, and S. Ramachandran, Optica **2**, 267 (2015).
23. M. E. V. Pedersen, P. Kristensen, L. Gruner-Nielsen, and K. Rottwitt, J. Lightwave Technol. **29**, 3129 (2011).
24. S. Ramachandran, IEEE Photon. Technol. Lett. **15**, 1171 (2003).
25. For instance, http://versawave.com/products/polarization-modulators/.
26. L. Novotny, M. R. Beversluis, K. S. Youngworth, and T. G. Brown, Phys. Rev. Lett. **86**, 5251 (2001).
27. K. S. Youngworth and T. G. Brown, Opt. Express **7**, 77 (2000).